HUMAN GENE THERAPY 23:742–753 (July 2012)

DOI: 10.1089/hum.2011.216

# Rapid Transgene Expression in Multiple Precursor Cell Types of Adult Rat Subventricular Zone Mediated by Adeno-Associated Type 1 Vectors

Olivier Bockstael,[1,2] Catherine Melas,[1,2] Catherine Pythoud,[3] Marc Levivier,[1,3] Douglas McCarty,[4,*] R. Jude Samulski,[4] Olivier De Witte,[1,5] and Liliane Tenenbaum[1–3]

## Abstract

The adult rat brain subventricular zone (SVZ) contains proliferative precursors that migrate to the olfactory bulb (OB) and differentiate into mature neurons. Recruitment of precursors constitutes a potential avenue for brain repair. We have investigated the kinetics and cellular specificity of transgene expression mediated by AAV2/1 vectors (i.e., adeno-associated virus type 2 pseudotyped with AAV1 capsid) in the SVZ. Self-complementary (sc) and single-stranded (ss) AAV2/1 vectors mediated efficient GFP expression, respectively, at 17 and 24 hr post-injection. Transgene expression was efficient in all the rapidly proliferating cells types, that is, Mash1$^+$ precursors (30% of the GFP$^+$ cells), Dlx2$^+$ neuronal progenitors (55%), Olig2$^+$ oligodendrocyte progenitors (35%), and doublecortin-positive (Dcx$^+$) migrating cells (40%), but not in the slowly proliferating glial fibrillary acidic protein-positive (GFAP$^+$) neural stem cell pool (5%). Because cell cycle arrest by wild-type and recombinant AAV has been described in primary cultures, we examined SVZ proliferative activity after vector injection. Indeed, cell proliferation was reduced immediately after vector injection but was normal after 1 month. In contrast, migration and differentiation of GFP$^+$ precursors were unaltered. Indeed, the proportion of Dcx$^+$ cells was similar in the injected and contralateral hemispheres. Furthermore, 1 month after vector injection into the SVZ, GFP$^+$ cells, found, as expected, in the OB granular cell layer, were mature GABAergic neurons. In conclusion, the rapid and efficient transgene expression in SVZ neural precursors mediated by scAAV2/1 vectors underlines their potential usefulness for brain repair via recruitment of immature cells. The observed transient precursor proliferation inhibition, not affecting their migration and differentiation, will likely not compromise this strategy.

## Introduction

The neurogenic pathway of the adult rat subventricular zone (SVZ) consists of several immature cell types at various stages of differentiation and with different proliferative rates: (1) slowly proliferative (type B) cells expressing glial fibrillary acidic protein (GFAP), (2) rapidly dividing "transit-amplifying" (type C) cells expressing Ascl1 (also called Mash1) and generating both Dlx2-positive neuronal progenitors and Olig2-positive oligodendrocyte progenitors (Kim *et al.*, 2007, 2011), and (3) migrating (type A) neuroblasts characterized by the expression of doublecortin (Dcx). It should be noted that Mash1/Ascl1, Dlx2, and Dcx marker expression in the progenitors is partially overlapping (Kim *et al.*, 2007). The latter progenitors migrate through the rostral migratory stream (RMS) to the olfactory bulb (OB) (Alvarez-Buylla and Garcia-Verdugo, 2002), where they differentiate into various types of mature neurons. By selective killing of type C cells or by cell fate mapping, it has been shown that type B cells are the ancestor of type C and type A cells (Doetsch *et al.*, 1999; Garcia *et al.*, 2004) and that type A neuroblasts and their descendant OB differentiated neurons originate from Ascl1 transit-amplifying type C progenitors (Kim *et al.*, 2007).

[1]Laboratory of Experimental Neurosurgery, Université Libre de Bruxelles, BE-1070 Brussels, Belgium.
[2]Multidisciplinary Research Institute, Université Libre de Bruxelles, BE-1070 Brussels, Belgium.
[3]Department of Clinical Neuroscience, University Hospital, CH-1011 Lausanne, Switzerland.
[4]Center for Gene Therapy, University of North Carolina at Chapel Hill, Chapel Hill, NC 27599.
[5]Department of Neurosurgery, Erasme Hospital, BE-1070 Brussels, Belgium.
*Present address: Children's Hospital, Columbus, OH 43062.

Gene transfer into SVZ neural stem cells before their migration has been proposed with the purpose of recruiting these cells for repair of CNS lesions (Fallon *et al.*, 2000; Chmielnicki *et al.*, 2004; Cho *et al.*, 2007; Henry *et al.*, 2007).

Retroviral and lentiviral vectors, which integrate into the cellular genome, have been used for tracing and fate analysis of SVZ neural stem cells (Smith and Luskin, 1998). Because of their requirement for cell division, retroviral vectors (Goldman *et al.*, 1993) have allowed the specific labeling of type C cells and, to a lesser extent, slowly proliferating GFAP-positive type B cells. Lentiviral vectors, which can infect both dividing and nondividing cells, were superior in transducing type B neural stem cells, hence ensuring long-term labeling of the whole pathway (Consiglio *et al.*, 2004; Geraerts *et al.*, 2006).

However, for therapeutic gene delivery, the use of a nonintegrative vector would be preferred in order to minimize the risk of insertional mutagenesis in dividing cells (Yanez-Munoz *et al.*, 2006). Recombinant AAV2/1 vectors (i.e., adeno-associated virus type 2 pseudotyped with AAV1 capsid) were previously shown to efficiently transduce cells of the SVZ, which later on to migrate to the OB (Wang *et al.*, 2003). However, the delay in obtaining detectable transgene expression in the brain, mediated by single-stranded rAAV2/1 vectors (ssAAV2/1), was shown to be 4 days postinjection (Reimsnider *et al.*, 2007). At this time point, a significant fraction of the initially infected cells is expected to have migrated away from the SVZ (Craig *et al.*, 1999). Self-complementary AAV (scAAV) vectors, which were shown to shorten the delay for transgene expression in the brain (McCarty *et al.*, 2001, 2003; McCarty, 2008), could constitute an interesting alternative.

Because inhibition of the proliferation of fibroblasts (Hermanns *et al.*, 1997; Kube *et al.*, 1997), keratinocytes (Alam *et al.*, 2006; Alam and Meyers, 2009), as well as grafted neural stem cell primary cultures (Wu *et al.*, 2002) by wild-type or recombinant AAV2 has been repeatedly documented, it was of interest to study the potential interactions between rAAV2/1 vectors and the proliferative cells present in adult brain neurogenic niches.

Therefore, in the present study, we have characterized the kinetics and cell type specificity of rAAV2/1-mediated gene transfer in the SVZ neurogenic niche as well as the proliferation, migration, and differentiation properties of transduced cells. Single-stranded AAV2/1 and scAAV2/1 vectors mediated detectable *gfp* transgene expression in the SVZ as early as 24 and 17 hr postinjection, respectively. All types of progenitors were transduced, with the largest proportion of green fluorescent protein (GFP)-positive cells harboring the Dlx2 marker of transit-amplifying neuronal progenitors. A partial (30%) inhibition of cell proliferation was observed in the transduced area shortly after virus infusion. This inhibitory effect was transient because, 1 month after vector injection, the number of proliferating cells was equivalent to that of the control. In addition, the percentage of migrating Dcx-positive neuroblasts as well as the localization and differentiation pattern of newly generated neurons in the OB were not altered.

## Materials and Methods

### *Plasmids and viruses*

Recombinant scAAV2/1 or ssAAV2/1 virus expressing the enhanced green fluorescent protein (eGFP)-encoding reporter gene under the control of the cytomegalovirus (CMV) promoter was produced by cotransfection of HEK-293T cells with pHpaItrs (McCarty *et al.*, 2003) or pTR-eGFP (Tenenbaum *et al.*, 1999), respectively, and pDP1rs (Grimm *et al.*, 2003) (purchased from Plasmid Factory, Heidelberg, Germany). Briefly, 3 $\mu$g of pTR-eGFP or pHpaItrs and 10 $\mu$g of pDP1rs were transfected into $5\times10^6$ cells (per 10-cm plate seeded 1 day previously) by the calcium phosphate coprecipitation method. The cell pellets from 20 plates were harvested, treated with Benzonase, and purified by iodixanol gradient followed by QXL chromatography (i.e., chromatography on Q Sepharose XL [GE Healthcare Life Sciences, Piscataway, NJ]) (Zolotukhin *et al.*, 1999). The virus was microconcentrated and diluted into Dulbecco's phosphate-buffered saline (D-PBS), using a Centriplus centrifugal concentrator (EMD Millipore, Billerica, MA).

Titers were measured by real-time PCR as described in www.isbiotech.org/ReferenceMaterials/pdfs/AAV2_RSS_genome_copy_titration_QPCR.pdf (International Society for BioProcess Technology, 2011).

Briefly, the method was first established with rAAV serotype 2 reference standard (Lock *et al.*, 2010). Viral particles were digested with DNase I at 10 U per 5 ml of virus diluted in 50 ml of DNase digestion buffer (13 m*M* Tris-HCl [pH 7.5], 5 m*M* $MgCl_2$, and 0.12 m*M* $CaCl_2$). Serial dilutions of the virus were subjected to qPCR, using qPCR master mix (Applied Biosystems/Life Technologies, Foster City, CA), forward primer 5′-AGCAATAGCATCACAAATTTCACAA-3′, reverse primer 5′-CCAGACATGATAAGATACATTGATGAGTT-3′, and internal fluorescent probe 6FAM-AGCATTTTTTTCACT GCATTCTAGTTGTGGTTTGTC-TAMRA (Eurogentec, Liège, Belgium). Titers, expressed as viral genomes per milliliter, were as follows: ssAAV2/1-CMV-eGFP, $4.3\times10^{11}$; scAAV2/1-CMV-eGFP, $2.1\times10^{10}$.

The amount of viral capsids in the ssAAV2/1-CMV-eGFP viral preparation was found to be $5.9\times10^{12}$ per milliliter (as evaluated by ELISA according to the recommendations of the manufacturer (Progen, Heidelberg, Germany).

### *Surgical procedures*

Adult female Wistar rats (250 g; Charles River, France) were used for unilateral intracerebral injections (Bockstael *et al.*, 2011). Briefly, the animals were anesthetized with a mixture of ketamine (Ketalar, 100 mg $kg^{-1}$, intraperitoneal) and xylazine (Rompun, 10 mg $kg^{-1}$, intraperitoneal) (Bayer, Leverkusen, Germany). Injections were made according to coordinates defined by Paxinos and Watson (1986), using a Kopf stereotaxic apparatus (David Kopf, Tujunga, CA). Viral particles diluted in 2 $\mu$l of D-PBS (Lonza Group, Basel, Switzerland) were infused into the medial part of the dorsal striatum, using a motor-driven Hamilton syringe (0.2 $\mu$l/min) equipped with a 30-gauge needle, at the following coordinates: anteroposterior (AP), 0 mm; lateral (L), −2.2 mm relative to bregma; and dorsoventral (DV), −4.2 mm relative to the cerebral surface (Paxinos and Watson, 1986). After injection, the needle was left in place for 5 min in order to allow diffusion of the viral suspension in the parenchyma. The needle was then slowly removed.

Animals were maintained, four in each cage, in a 12:12 hr light–dark cycle with free access to rat chow and water. Experimental procedures were conducted with the approval of the Belgium Biosafety Advisory Committee and the ethics

committee of the Faculty of Medicine (Commission d'Ethique du Bien-Être Animal [CEBEA], Université Libre de Bruxelles [ULB]).

Animals were killed with an overdose of anesthetic (ketamine, 200 mg $kg^{-1}$; and xylazine, 20 mg $kg^{-1}$) at the indicated time after virus injection. For immunohistological analysis, animals were perfused through the ascending aorta first with 150–200 ml of saline (0.9% NaCl), and then with 200 ml of 4% paraformaldehyde in 0.1 *M* phosphate buffer (PF4). After overnight fixation in PF4 at 4°C, brains were transferred to PBS and stored at 4°C.

### *5-Bromo-2′-deoxyuridine-5′-monophosphate*

When indicated, 5-bromo-2′-deoxyuridine-5′-monophosphate (BrdU, 20 mg $kg^{-1}$; Sigma-Aldrich, St. Louis, MO) was injected intraperitoneally twice per day.

To determine the proliferative index, BrdU (20 mg $kg^{-1}$) was injected three times intraperitoneally, that is, 20, 4, and 2 hr before surgery. BrdU (1 mg $ml^{-1}$) was also given in drinking water containing sucrose (30 g $liter^{-1}$) during the night before surgery (from 20 to 4 hr before surgery).

### *Immunohistochemistry*

For GFP staining, vibrating blade microtome sections (50 $\mu$m) were sequentially incubated (1) for 30 min in 3% $H_2O_2$ in TBS (10 m*M* Tris, 0.9% NaCl; pH 7.6), (2) for 1 hr in THST (50 m*M* Tris, 0.5 *M* NaCl, 0.5% Triton X-100; pH 7.6) containing 10% horse serum, (3) overnight at 4°C with polyclonal rabbit anti-GFP (Clontech, Palo Alto, CA) diluted 1:3000 in THST containing 5% horse serum, and (4) for 2 hr at room temperature with donkey anti-rabbit IgG conjugated with biotin (Amersham/GE Healthcare, Munich, Germany) diluted 1:600 in THST containing 5% horse serum. The peroxidase staining was revealed with an VECTASTAIN Elite ABC kit and diaminobenzidine (Vector/NTL Laboratories, Brussels, Belgium), according to the manufacturer's protocol. Sections were mounted on gelatin-coated slides, dehydrated, and mounted with DPX mounting fluid (Sigma-Aldrich). Sections were photographed with a Zeiss Axiophot 2 microscope (Carl Zeiss, Göttingen, Germany).

To determine transduction volumes, surfaces of labeled SVZ were first evaluated (every fifth section) with the AxioVision program (version 4.7.1; Carl Zeiss). Volumes ($\mu m^3$) were calculated by adding the surfaces of positive sections and multiplying by the section thickness (50 $\mu$m) and by 5.

### *Immunofluorescence*

Coronal sections (50 $\mu$m) obtained with a vibrating blade microtome (Leica Microsystems, Wetzlar, Germany) were sequentially incubated (1) for 2 hr in THST containing 10% horse serum, (2) for 16 hr at 4°C with polyclonal rabbit anti-GFP IgG (Molecular Probes/Life Technologies, Eugene, OR) diluted 1:3000 in THST containing 5% horse serum, (3) for 2 hr at room temperature with biotin-conjugated donkey anti-rabbit IgG (Amersham/GE Healthcare) diluted 1:600 in THST containing 5% horse serum, and (4) for 2 hr at room temperature with streptavidin-conjugated cyanine 2 (Cy2; Jackson ImmunoResearch, West Grove, PA) diluted 1:300 in THST containing 5% horse serum. Three washings in TBS (10 min each) were performed between each step.

For double immunofluorescence against NeuN (neuronal nuclear antigen; mature neurons), glutamic acid decarboxylase-67 (GAD67; GABAergic neurons), and GFAP (astrocytes and neural stem cells), GFP immunofluorescence was combined with mouse monoclonal anti-NeuN (diluted 1:200; Chemicon/EMD Millipore), mouse monoclonal anti-GAD67 (diluted 1:500; Chemicon/EMD Millipore), or mouse monoclonal anti-glial fibrillary acid protein (GFAP, diluted 1:200; Chemicon/EMD Millipore) antibodies followed by donkey anti-mouse IgG coupled to cyanine 3 (Cy3, diluted 1:200; Jackson ImmunoResearch) in THST containing 5% horse serum.

For double immunofluorescence directed against Dcx (migrating cells), GFP immunofluorescence was combined with guinea pig polyclonal antibody anti-Dcx (diluted 1:300; Chemicon/EMD Millipore) followed by donkey anti-guinea pig IgG coupled to Cy3 (diluted 1:200; Jackson ImmunoResearch) in THST containing 5% horse serum.

For double immunofluorescence directed against GFP and Olig2 (oligodendrocyte progenitors), a chicken monoclonal anti-GFP antibody (Abcam, Cambridge, UK) at a 1:1000 dilution was combined with rabbit polyclonal anti-Olig2 IgG (diluted 1:500; Chemicon/EMD Millipore) in PBS containing 5% horse serum and 0.1% Triton X-100 and incubated for 16 hr at 4°C. The primary antibodies were detected with biotin-conjugated donkey anti-rabbit IgG (diluted 1:200; Amersham/GE Healthcare) and a goat anti-chicken IgG conjugated with Alexa 488 (diluted 1:1000; Molecular Probes/Life Technologies) in PBS containing 5% horse serum and 0.1% Triton X-100, 2 hr at room temperature, and then incubated with streptavidin coupled to Cy3 (diluted 1:600; Jackson ImmunoResearch) in PBS containing 5% horse serum and 0.1% Triton X-100, 2 hr at room temperature.

For double immunofluorescence directed against GFP and Dlx2, a chicken monoclonal anti-GFP antibody (Abcam) at a 1:1000 dilution was combined with rabbit anti-Dlx2 IgG (ab30339, diluted 1:200; Abcam) followed by a Cy3-coupled donkey anti-rabbit IgG (diluted 1:500; Jackson ImmunoResearch).

For double immunofluorescence directed against GFP and Mash1, GFP immunofluorescence was combined with a mouse anti-Mash1 IgG1 (clone 24B72D11.1, diluted 1:100; BD Biosciences, San Jose, CA) followed by a biotinylated rat anti-mouse IgG1 (clone A85-1, diluted 1:200; BD Biosciences) and streptavidin coupled to Cy3 (diluted 1:200; Jackson ImmunoResearch).

For BrdU immunofluorescence, sections were first treated as follows to allow the antibody to reach the nucleus: sections were incubated with 1 *N* HCl for 10 min on ice, transferred to 2 *N* HCl for 10 min at room temperature, and then further incubated at 37°C for 20 min. Sections were then transferred into sodium borate (0.1 *M*, pH 8.5) for 15 min.

For BrdU/GFP and BrdU/Ki67 double immunofluorescence, a rat monoclonal anti-BrdU antibody (diluted 1:200; Abcam) was combined with rabbit polyclonal anti-GFP (diluted 1:3000; Molecular Probes) or rabbit polyclonal anti-Ki67 (diluted 1:500; Novocastra, Newcastle upon Tyne, UK) antibody in THST containing 5% horse serum, 16 hr at 4°C. A goat anti-rat IgG coupled to Cy3 (diluted 1:600; Jackson ImmunoResearch) was used to detect anti-BrdU primary antibodies. A goat anti-rabbit IgG coupled to biotin (diluted 1:500; Jackson ImmunoResearch) followed by incubation in streptavidin coupled to Alexa 647 (diluted 1:500; Jackson ImmunoResearch) was used to detect anti-Ki67 primary

antibodies. Alternatively, a goat anti-rabbit IgG coupled to biotin (diluted 1:500; Jackson ImmunoResearch) followed by incubation in streptavidin coupled to Cy2 (diluted 1:500; Jackson ImmunoResearch) was used to detect anti-GFP primary antibodies.

For nuclear counterstainings, sections were incubated for 30 min with Hoechst 33258 dye (Sigma-Aldrich) diluted to 1 $\mu$g/ml in TBS.

Three washings in TBS of 10 min were performed between each step.

Sections were mounted on gelatin-coated slides, using Glycergel mounting fluid for fluorescence (Dako, Glostrup, Denmark).

### *Confocal microscopy*

Colabeling and proliferative index analyses were performed on pictures taken of at least three different sections, using an LSM 510 NLO multiphoton confocal microscope fitted on an Axiovert M200 inverted microscope equipped with C-Apochromat ×40/1.2 NA water immersion objectives (Carl Zeiss, Jena, Germany).

The 488-nm excitation wavelength of the Argon II laser, a main dichroic HFT 488 beam splitter, and a bandpass emission filter (BP500–550 nm) were used for selective detection of the green fluorochrome (Cy2). The 543-nm excitation wavelength of the HeNe1 laser, a main dichroic HFT 488/543/633 beam splitter, and a long-pass emission filter (BP565–615 nm) were used for selective detection of the red fluorochrome (Cy3). The 633-nm excitation wavelength of the HeNe2 laser, a main dichroic HFT 488/543/633 beam splitter, and a long-pass emission filter (BP650–700 nm) were used for selective detection of the far-red fluorochrome (Alexa 647). The nuclear stain Hoechst/DAPI was excited in multiphotonic mode at 760 nm with a Mai Tai tunable broadband laser (Spectra-Physics, Darmstadt, Germany) and detected with a main dichroic HFT KP650 beam splitter and a bandpass emission filter (BP435–485 nm).

Optical sections (2 $\mu$m thick, 512 by 512 pixels) were collected sequentially for each fluorochrome. *Z*-stacks with a focus step of 1 $\mu$m were collected.

The data sets generated were merged and displayed with Zeiss ZEN 2009 software and exported in LSM image format.

Countings were performed with ImageJ 1.46a software (National Institutes of Health, Bethesda, MD). Figures were prepared with Adobe Photoshop CS3 software (Adobe, San Jose, CA).

### *Proliferative index*

The proliferative index is the ratio of the number of proliferating cells (detected by expression of Ki67 protein) to the number of cells previously in proliferation, measured by the incorporation of BrdU during a given time lapse.

### *Apoptosis detection*

To evaluate apoptosis induction, an *in situ* cell death detection kit (Roche Applied Science, Indianapolis, IN) was used according to the manufacturer's recommendations.

Briefly, the animals were killed by decapitation 24 hr after surgery, after the injection of an overdose of anesthetic (ketamine, 200 mg $kg^{-1}$; and xylazine, 20 mg $kg^{-1}$). The brains were rapidly frozen to −20°C, using dry ice in a bath of methylbutane, and then stored at −80°C. Cryosections (16 $\mu$m thick) were made with a Leica cryostat and placed on Superfrost Plus slides. Terminal deoxynucleotidyltransferase-mediated dUTP nick end-labeling (TUNEL) detection was done with the *in situ* cell death detection kit (Roche Applied Science) according to the manufacturer's recommendations for difficult tissues. TUNEL-positive cells were quantified with a Zeiss Axiophot 2 microscope equipped with fluorescein isothiocyanate (FITC) and tetramethylrhodamine isothiocyanate (TRITC) filters (Carl Zeiss, Göttingen, Germany) on five sections surrounding the injection site, covering 400 $\mu$m along the anteroposterior axis. Cells were counted in the SVZ ipsilateral and contralateral to the injection site. Ipsilateral counts were divided by contralateral counts to normalize small anteroposterior differences between animals.

### *Statistical analyses*

Means ± standard deviations are shown. Data were analyzed using Prism 3.0 software (Graph Pad Software, San Diego, CA). Unpaired Student *t* tests and one-way analysis of variance (ANOVA) were performed.

### *Virus irradiation*

ssAAV2/1-CMV-eGFP diluted in D-PBS (Lonza Group) was irradiated with a UV Stratalinker chamber (Stratagene/Agilent Technologies, La Jolla, CA) at a dose of 4800 J/$m^2$. Irradiation completely abolished GFP expression as assessed by infection of HEK-293T cells and fluorescence-activated cell-sorting (FACS) analysis.

### *Bovine serum albumin injections*

Protein concentration of the stock of ssAAV2/1-CMV-eGFP, measured with a Micro BCA protein assay kit (Pierce/Thermo Fisher Scientific, Rockford, IL) according to the manufacturer's recommendations, was found to be 20 $\mu$g/ml. A solution of bovine serum albumin (BSA) diluted to 20 $\mu$g/ml in D-PBS was injected in the vicinity of the SVZ according to the method described above for viral injections (see surgical procedures).

## Results

### *Fast and efficient transduction of subventricular zone neural precursors by rAAV2/1*

It has been previously reported that injection of rAAV2/1 vectors using the CMV promoter into the striatum of mice (Passini *et al.*, 2003; Wang *et al.*, 2003) and rats (Bockstael *et al.*, 2008) resulted in efficient transduction of the SVZ. In these studies, GFP-positive cells were found in the OB, the region in which neural stem cells of the SVZ terminally differentiate.

Because of the rapid dynamics of the SVZ–OB pathway, most type C progenitors and type A neuroblasts are expected to have migrated away in the RMS within a few days (Craig *et al.*, 1999). Therefore, we evaluated transduction efficiency of self-complementary and single-stranded AAV2/1 vectors during the first 4 days after injection of $4.3 \times 10^7$ genome copies (low dose) of each virus into the medial part of the

dorsal striatum (Fig. 1a). Transduction efficiency was evaluated immunohistochemically as the volume of SVZ staining positive for GFP (Fig. 1b).

scAAV2/1 transduced the SVZ as early as 17 hr after vector injection, and maximal transduction efficiency was reached at 24 hr (Fig. 1b). In contrast, ssAAV2/1-transduced cells in the SVZ were detected only 24 hr postinjection, and the highest efficiency was reached at 48 hr (Fig. 1b). Transduction decreased at 96 hr, the decrease being more pronounced for the ssAAV2/1 vector (Fig. 1b), and was low at 1 month (data not shown). Increasing the amount of ssAAV2/1 by 20-fold ($8.6\times10^8$ genome copies, high dose) did not result in a significant improvement of transduction efficiency (Fig. 1b).

### *Characterization of rAAV2/1-transduced cells in the subventricular zone*

During their commitment from neural stem cells to mature neurons, immature cells express various and sometimes overlapping markers (Kim *et al.*, 2007; Jones and Connor, 2011). To characterize the cellular specificity of rAAV2/1-mediated transgene expression, animals were killed 2 days after injection of vectors in the vicinity of the SVZ (at the time at which the number of $GFP^+$ cells is maximal for both vectors). Vibrating blade microtome sections were subjected to double immunofluorescence for GFP and, respectively, GFAP (labeling slowly proliferating type B cells), Mash1 (labeling rapidly proliferating type C cells), Dlx2 (labeling

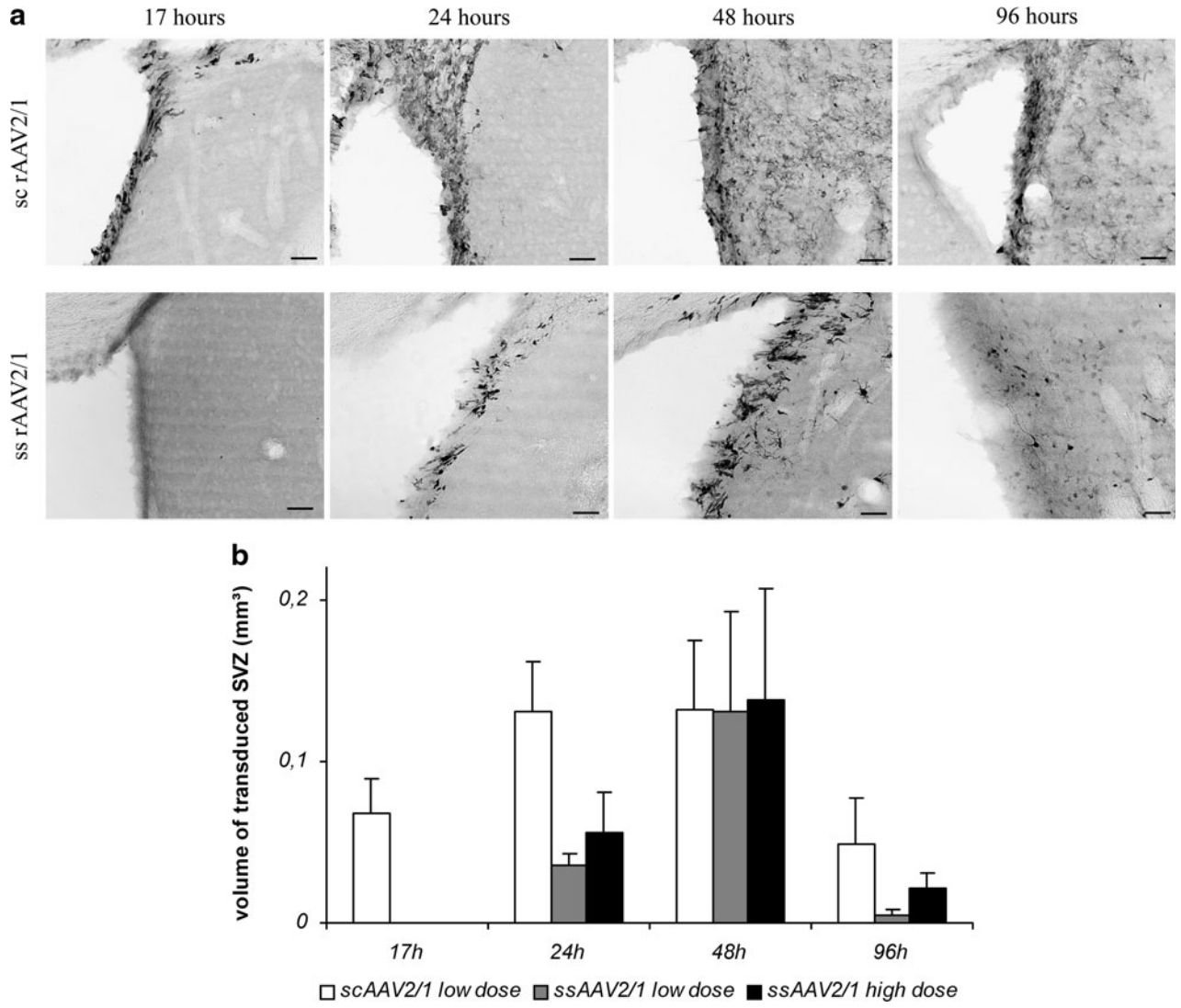


**FIG. 1.** Transduction of the subventricular zone by rAAV2/1. A low dose of scAAV2/1-CMV-eGFP or ssAAV2/1-CMV-eGFP or a high dose of ssAAV2/1 was injected into the medial striatum. **(a)** Seventeen, 24, 48, and 96 hr after injection of a low dose of the indicated vector, 50-$\mu$m vibrating blade microtome sections were labeled with anti-GFP antibodies and photographed with a Zeiss Axioplan 2 microscope and a $\times20$ objective (scale bars, 250 $\mu$m). **(b)** Transduction volumes after injection of a low dose of scAAV2/1 (open columns), a low dose of ssAAV2/1 (gray columns), and a high dose of ssAAV2/1 (solid columns) were quantified by the AxioVision program to evaluate the GFP-positive surfaces in the subventricular zone (SVZ) and multiplying by the thickness of the sections (50 $\mu$m) and the number of sections between two counted sections (five) (see Materials and Methods).

rapidly proliferating type C neuronal precursors subpopulation), Olig2 (labeling a rapidly proliferating type C oligodendrocyte precursor sub-population), or doublecortin (Dcx, labeling migrating type A neuroblasts) (Fig. 2a).

As shown in Fig. 2b, 2 days postinjection of ssAAV2/1 ($n=4$), 29.09 ± 3.23% of GFP$^+$ cells in the SVZ (as delineated by Hoechst 33258 staining; data not shown) were Mash1$^+$, 57.7 ± 9.92% were Dlx2$^+$, and 36.97 ± 6.9% were Olig2$^+$, 44.71 ± 2.08% were Dcx$^+$, whereas only 5.85 ± 0.45% were GFAP$^+$. Similar proportions of Mash1$^+$ cells (27.49 ± 3.58%, $n=4$, $p=0.532$, Student $t$ test), Dlx2$^+$ cells (52.28 ± 3.01%, $n=3$, $p=0.1974$, Student $t$ test), Olig2$^+$ cells (29.41 ± 7.64 %, $n=7$, $p=0.1379$, Student $t$ test), and GFAP$^+$ cells (4.69 ± 1.46%, $n=4$, $p=0.1792$, Student $t$ test) were transduced by the scAAV2/1 vector. Proportions of GFP$^+$ cells expressing Dcx were significantly different ($p=0.007$, Student $t$ test) between

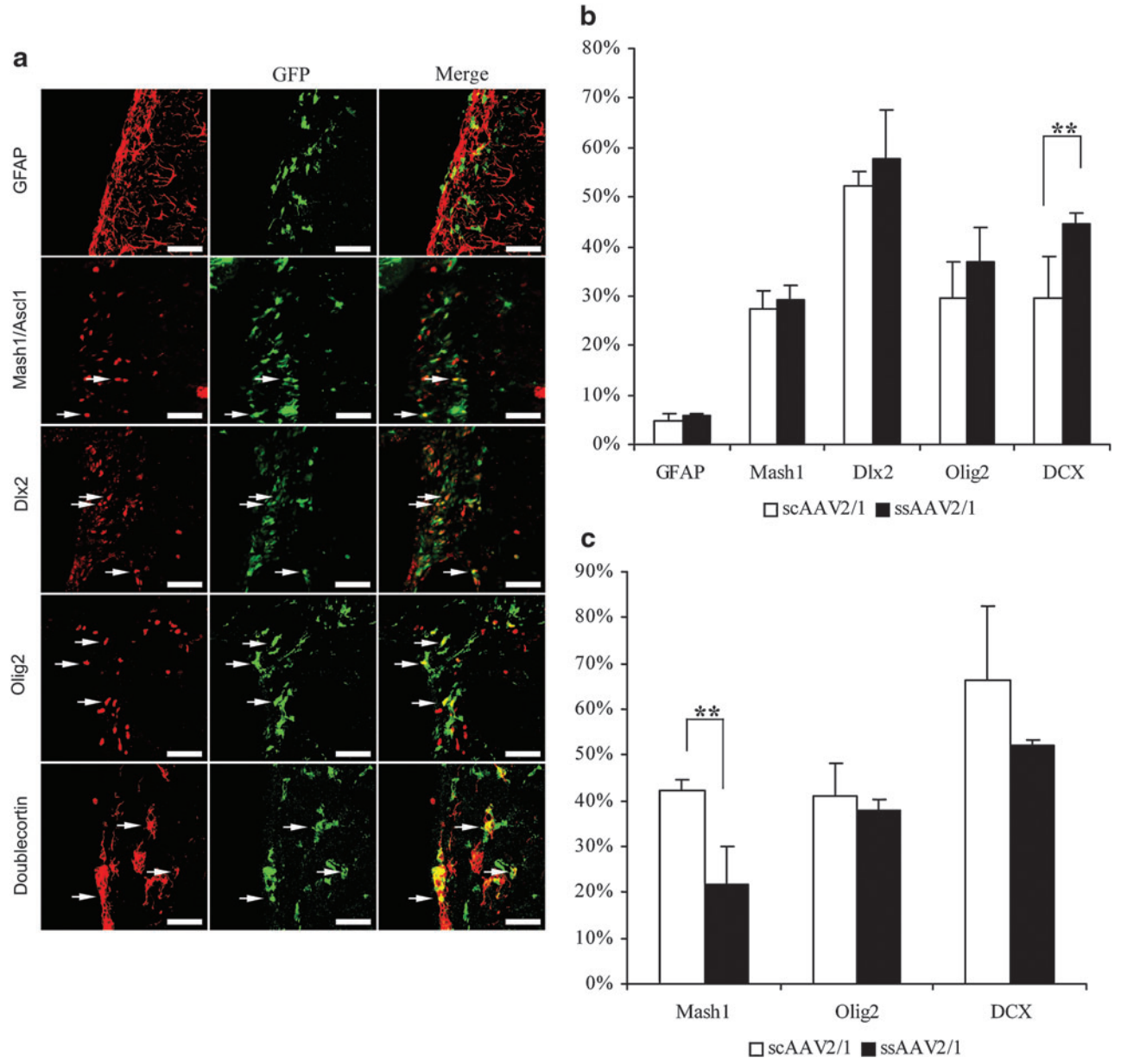


**FIG. 2.** Characterization of scAAV2/1-CMV- and ssAAV2/1-CMV-eGFP-transduced cells in the adult SVZ. Two days after injection of scAAV2/1-CMV-eGFP and ssAAV2/1-CMV-eGFP (low dose) into the medial striatum, 50-$\mu$m vibrating blade microtome sections of the forebrain were colabeled with anti-GFP (green fluorescence) and anti-GFAP, anti-Mash1, anti-Dlx2, anti-Olig2, or anti-Dcx (red fluorescence) antibodies. **(a)** Confocal pictures show GFP and cell-specific markers in double-labeled cells (yellow) 2 days after scAAV2/1-CMV-eGFP (low dose) injection. Arrows indicate double-labeled cells. Scale bars, 50 $\mu$m. **(b)** The proportions of colabeled cells relative to the total number of GFP$^+$ cells were significantly different between the two vectors for doublecortin but not for the GFAP, Mash1, Dlx2, or Olig2 markers. **(c)** The proportions of colabeled cells relative to the total number of specific progenitor marker-positive cells were significantly different between the two vectors for Mash1 but not for the Olig2 or doublecortin markers. Open columns, scAAV2/1-CMV-eGFP; solid columns, ssAAV2/1-CMV-eGFP. Data are expressed as means ± SD. **$p<0.01$.

ssAAV2/1-injected animals and scAAV2/1-injected animals (44.7 ± 2.1% [$n = 4$] and 29.64 ± 8.33% [$n = 7$], respectively).

### *Efficacy of rAAV2/1-mediated gene transfer into SVZ progenitors*

To determine the efficacy of both scAAV2/1 and ssAAV2/1 to mediate gene transfer into SVZ progenitor cells, we quantified the proportion of specific progenitor subtypes also expressing GFP in the transduced area (only sections harboring GFP-positive cells, corresponding to approximately 30% of the complete SVZ, were taken into account).

As shown in Fig. 2c, 48 hr after injection of scAAV2/1, 42.13 ± 2.4% of Mash1$^+$ cells also express GFP ($n = 4$), 41.12 ± 7.19% of Olig2$^+$ cells were also GFP$^+$ ($n = 7$), and 66.39 ± 16.23% of DCX$^+$ cells also express GFP ($n = 8$). Similar proportions of Olig2$^+$ cells and DCX$^+$ cells were found to express GFP (37.91 ± 2.55%, $n = 4$, $p = 0.4183$, Student $t$ test and 52.2 ± 1.21%, $n = 4$, $p = 0.1192$, Student $t$ test, respectively) 2 days after ssAAV2/1 injections (low dose) whereas Mash1$^+$ cells were less efficiently transduced by ssAAV2/1 than by scAAV2/1 (21.62 ± 8.25%, $n = 4$, $p = 0.0031$, Student $t$ test).

Because of their high density (see Fig. 2a), reliable counting of Dlx2$^+$ neuronal progenitors was unfeasible.

### *Inhibition of SVZ proliferative activity by rAAV2/1 virus*

Because BrdU is incorporated mainly by transit-amplifying type C cells, it is expected that when Dlx2$^+$ transduced cells migrate to the OB and differentiate into postmitotic neurons, they will still harbor BrdU in their genome. We thus searched for BrdU/GFP double-labeled cells in the OB 5 weeks after injection of $4.3 \times 10^7$ genomes of ssAAV2/1 and BrdU injections at various time points (Fig. 3a).

When BrdU was administered for 5 days starting 5 days before virus injection, 83.12 ± 11.07% of the GFP$^+$ cells found in the OB 5 weeks later were colabeled with anti-BrdU antibodies ($n = 4$). In contrast, when BrdU was injected for 5 days starting immediately after virus injection, a highly significant decrease in GFP-expressing cells colabeling with BrdU (10.5 ± 6.21%, $n = 4$, $p < 0.0001$, Student $t$ test; Fig. 3a) was observed.

In contrast, the overall BrdU-labeled cell density in the OB 5 weeks after virus injection was similar in both groups ($p = 0.5124$, Student $t$ test; data not shown). This means that the observed drastic reduction in BrdU labeling in GFP$^+$ cells in the OB is not related to the BrdU delivery time schedule but to the rAAV2/1 infection.

To further assess the effect of rAAV2/1 on SVZ progenitor proliferation, the proliferative index of the SVZ was measured 24 hr after vector injection. We observed a highly significant ($p < 0.0001$, one-way ANOVA) decrease in the ratio of Ki67$^+$ versus BrdU$^+$ cells in the SVZ after injection of $4.3 \times 10^7$ viral genomes of ssAAV2/1-CMV-eGFP ($n = 7$) or scAAV2/1-CMV-eGFP ($n = 5$) compared with animals injected with vehicle (D-PBS, $n = 10$): respectively, 87.69 ± 7.4%, 89.18 ± 4.2%, and 131.12 ± 16.87% (Fig. 3b).

### *rAAV2/1 virus does not increase apoptosis in the SVZ*

Cell numbers in the SVZ are known to be controlled by a low level of apoptosis (Ricard *et al.*, 2006). To assess whether the observed reduction of the proliferative index could be

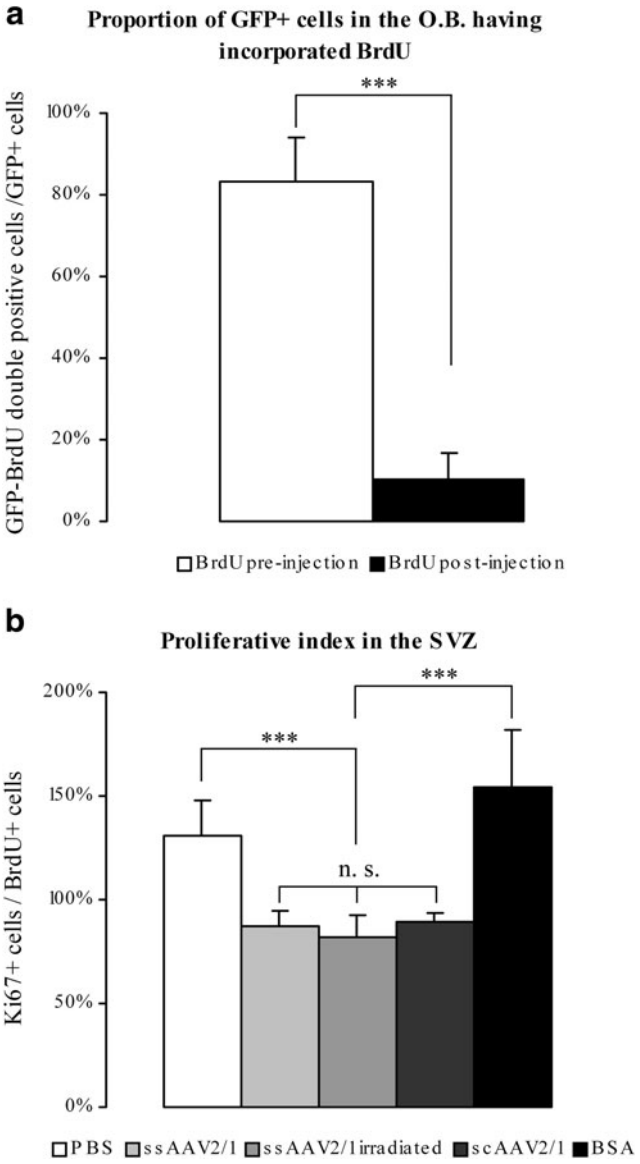


**FIG. 3.** Inhibition of SVZ proliferative activity by rAAV2/1. **(a)** Five weeks after injection of ssAAV2/1-CMV-eGFP (low dose) into the medial striatum, a significantly different proportion of double-labeled cells positive for GFP and BrdU relative to the total number of GFP$^+$ cells was found in the OB of animals receiving BrdU for 5 days before virus injection or immediately after vector injection. Open column, BrdU preinjection; solid column, BrdU postinjection. **(b)** The proliferative index of the SVZ was measured around the injection site 24 hr after injection of virus diluent buffer (sham injection), ssAAV2/1-CMV-eGFP, irradiated ssAAV2/1-CMV-eGFP, scAAV2/1-CMV-eGFP, or 0.4 $\mu$g of unspecific proteins close to the SVZ. A significant reduction in the proliferative index was found between the sham-injected group and the other groups and between the BSA-injected group and the other groups. No significant difference was found between the ssAAV2/1-CMV-eGFP-injected animals, the irradiated ssAAV2/1-CMV-eGFP-injected animals, and the scAAV2/1-CMV-eGFP-injected animals or between the sham-injected group and the BSA-injected group. Data are expressed as means ± SD. ***$p < 0.0001$.

due to increased apoptotic neural precursor cell death, TUNEL fluorescence staining of the SVZ was performed shortly (24 hr) after rAAV2/1 injection. As expected, few TUNNEL-positive cells were observed in the SVZ. However, there was no significant difference ($p = 0.3827$, Student $t$ test, data not shown) between the ratio of TUNEL-positive nuclei observed ipdsilateral and contralateral to the injection side of virus injected ($n = 5$) and sham (D-PBS)-injected animals $n = 4$). Let us notice that numerous positive nuclei were observed around the needle track of both virus- and PBS-injected animals. As expected DNase-treated sections (positive control) harboured positive nuclei on the whole sections.

### *Proliferation inhibition in the SVZ does not require vector-derived protein synthesis*

To evaluate the contribution of transgene expression to this effect, $5.9 \times 10^8$ viral capsids (corresponding to $4.3 \times 10^7$ viral genomes) of UV-irradiated ssAAV2/1-CMV-eGFP ($4800\,J/m^2$) were injected in the vicinity of the SVZ. (*Note:* The UV-irradiated virus did not express GFP, as demonstrated by the absence of green fluorescent cells after infection of etoposide-treated HEK-293T cells; data not shown.) A similar drop in the proliferative index ($p > 0.05$, one-way ANOVA test) as with nonirradiated virus was observed ($81.68 \pm 11.29\%$, $n = 4$; Fig. 3b).

### *Proliferation inhibition in the SVZ is not due to unspecific high protein loads*

To evaluate the contribution of a high amount of protein to this proliferation inhibition effect, 0.4 $\mu$g (corresponding to the capsid protein concentration of the low-dose virus) of unspecific proteins (BSA) was injected in the vicinity of the SVZ. The proliferative indexes observed in the SVZ of the BSA-injected animals ($154.46 \pm 27.07\%$, $n = 4$) and D-PBS-injected animals ($131.12 \pm 16.87\%$, $n = 10$) were similar ($p > 0.05$, one-way ANOVA test; Fig. 3b).

### *Proliferation inhibition in the SVZ is transient*

The proliferative index is not suitable to assess the effect of AAV2/1 injection on SVZ proliferation at later time points since most BrdU-labeled cells have presumably migrated away through the rostral migratory stream toward the OB. We therefore injected a single pulse of BrdU (20 mg/kg, intraperitoneal) 4 weeks after virus injection and killed the animals 24 hr later. $BrdU^+$ cell density was then calculated in the ipsilateral and contralateral SVZ on three sections covering 500 $\mu$m along the anteroposterior axis around the injection point. No significant difference was found ($p = 0.532$, Student $t$ test; data not shown) between ipsilateral and contralateral $BrdU^+$ cell density in the SVZ, indicating that the proliferation rate of the SVZ had returned to normal 4 weeks after virus injection.

### *rAAV2/1 transduction of SVZ neural progenitors does not modify the proportion of migrating neuroblasts in the SVZ*

To evaluate the effect of AAV2/1 injection on the phenotype of subventricular progenitors, we counted the number of $Dcx^+$ cells in the injected SVZ and in the contralateral SVZ. $Dcx^+$ cell counts were normalized by $Mash1^+/Ascl1^+$ cell numbers observed on adjacent sections. No difference was found between the proportions of $Dcx^+$ cells on the injected versus the contralateral side ($p = 0.2978$; data not shown), suggesting that AAV2/1 did not bias progenitor fate.

### *rAAV2/1 transduction of SVZ neural progenitors does not modify their terminal localization and differentiation into the OB*

It has been previously shown that most SVZ precursors give rise to neurons of the OB granule cell layer, whereas OB periglomerular neurons derive from RMS precursors (Hack *et al.*, 2005). Granule neurons are almost exclusively GABAergic whereas among periglomerular neurons, only 40% are GABAergic (Parrish-Aungst *et al.*, 2007).

Five weeks after injection of $4.3 \times 10^7$ viral genomes of ssAAV2/1-CMV-eGFP ($n = 5$) or scAAV2/1-CMV-eGFP ($n = 4$) close to the SVZ, GFP-positive cells were present in the OB granule cell layer. The vast majority of transduced cells were $NeuN^+$ ($90.62 \pm 3.93\%$ and $86.46 \pm 3.69\%$ for ssAAV2/1 and scAAV2/1, respectively; Fig. 4a). As expected for newly generated neurons originating from the periventricular area (Kosaka *et al.*, 1995), the majority of $GFP^+$ cells were GABAergic, as shown by the colocalization with GAD67

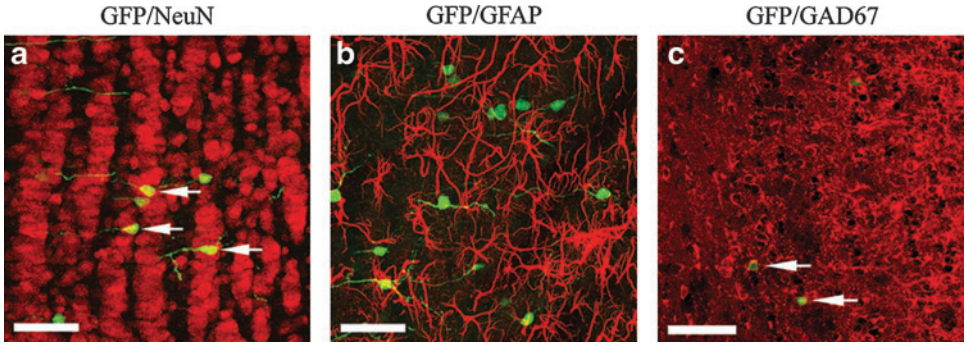


**FIG. 4.** Characterization of transduced cells in the olfactory bulb after injection of rAAV2/1 into the medial striatum. Five weeks after injection of ssAAV2/1-CMV-eGFP (low dose) close to the SVZ, 50-$\mu$m vibrating blade microtome sections of the olfactory bulbs were colabeled with anti-GFP (green fluorescence) and anti-NeuN **(a)**, anti-GFAP **(b)**, or anti-GAD67 **(c)** (red fluorescence) antibodies. Double-labeled cell bodies (yellow) were evidenced by confocal microscopy. Arrows indicate double-labeled cells. Scale bars: 50 $\mu$m.

(84.43 ± 3.18% and 82.07 ± 6.42% for ssAAV2/1 and scAAV2/1, respectively; Fig. 4c), and tyrosine hydroxylase (TH) negative (data not shown). No GFP/GFAP-colabeled cells were identified for either vector (Fig. 4b).

## Discussion

It has been shown that rAAV2/1 vectors efficiently and rapidly transduced neuronal progenitors of the adult rat SVZ at various stages of their commitment: multipotent Mash1$^+$ neural precursors, Dlx2$^+$ neuronal progenitors, and Dcx$^+$ migrating neuroblasts. Oligodendroglial progenitors were also transduced but less efficiently. In contrast, the pool of GFAP$^+$ neural stem cells was poorly transduced. These data are important for strategies aiming at the transient recruitment of neuronal progenitors for brain repair (Fallon *et al.*, 2000; Chmielnicki *et al.*, 2004; Cho *et al.*, 2007) without affecting the long-term normal function of the SVZ–OB pathway. Furthermore, transgene expression started early after vector injection, that is, 24 hr for single-stranded (ss) AAV2/1 and 17 hr for self-complementary (sc) AAV2/1, a delay that is compatible with the genetic modification of progenitors before these migrate en route to the OB. These results are in contrast with a previously published study showing that neural progenitors isolated from fetal brain and cultured as neurospheres are poorly susceptible to AAV-mediated gene transfer (Hughes *et al.*, 2002). However, cultured fetal neural progenitors and adult neural progenitors *in situ* in the SVZ environment could differ in terms of receptor expression, proliferative state, and so on. Furthermore, AAV2/1 has not been tested in this study. Notably, in another more recent study, AAV6, which differs from AAV1 by only six amino acids (Ng *et al.*, 2010), mediated GFP expression in 10% of cultured neural progenitors whereas AAV2 and AAV5 provided low (1%) efficiency.

A slow onset of transgene expression mediated by rAAV vectors in the brain has been frequently described (Duan *et al.*, 2000; McCown, 2005). This delay was suggested to reflect limiting steps such as viral particle intracellular trafficking (Duan *et al.*, 2000), uncoating of the virion (Thomas *et al.*, 2004), and second-strand synthesis (Ferrari *et al.*, 1996; Fisher *et al.*, 1996). With the aim to transfer genes into neural progenitors, which leave the SVZ and migrate through the RMS within a few days (Craig *et al.*, 1999), a vector able to rapidly transduce these cells is required. Reimsnider and colleagues (2007) have shown that rAAV2/1 mediates efficient transgene expression in the striatum as early as 4 days after injection and that the number of GFP-immunoreactive cells observed at 4 days was equivalent to that observed at later time points (up to 9 months). In the present report, transduction efficiency of SVZ cells peaked as early as 24 and 48 hr postinjection of scAAV2/1 and ssAAV2/1 vectors, respectively. This faster onset of expression observed in SVZ precursors as compared with the striatum (present study, Fig. 1) (Reimsnider *et al.*, 2007) could be related to the proliferative state of the target cell population (Halbert *et al.*, 1995). However, in contrast to the study by Halbert and colleagues, using immortalized cell lines, another report using muscle primary cultures suggests that the proliferative status does not affect short-term gene transfer efficiency (Malik *et al.*, 2000).

Self-complementary vectors have been demonstrated to allow faster onset and higher efficiency of transgene expression in the brain (McCarty *et al.*, 2003; McCarty, 2008). Accordingly, in the present study, the delay in transgene expression within the SVZ was longer for ssAAV2/1 than for scAAV2/1, suggesting that second-strand synthesis is a limiting step.

Globally at 48 hr postinjection, both vectors mediate similar efficiency of transgene expression. However, when the various cell types are examined separately, scAAV2/1 and ssAAV2/1 mediate similar efficiency of gene transfer in Dcx$^+$ (66 vs. 52%, NS) and Olig2$^+$ (41 vs. 38%, NS) cells but, in contrast, the proportion of Mash1$^+$ cells expressing GFP was significantly higher with the self-complementary vector (42 vs. 22%; $p < 0.005$). These data could suggest that second-strand synthesis is more limiting in Mash1$^+$ cells than in the other progenitor types because a cellular factor required for second-strand synthesis is present in more limiting amounts in these cells. Alternatively, it could be that in highly proliferative Mash1$^+$ cells, in which vector genomes are expected to be rapidly diluted, the limiting genome copy number necessary to obtain detectable transgene expression is more rapidly reached with single-stranded AAV than with self-complementary AAV. In contrast, there is no difference between both vectors in terms of the numbers of GFP$^+$ cells present in the olfactory bulb 1 month postinjection. Altogether, these data suggest that both vectors differ regarding the onset but not the long-term stability of transgene expression.

The observed reduced proportion of Dcx$^+$ cells among total GFP$^+$ cells with scAAV2/1 as compared with ssAAV2/1 at 48 hr, as well as the slight tendency for reduced proportions of double-labeled cells expressing Mash1, Dlx2, and Olig2 markers, could reflect efficient transgene expression in differentiated brain cells with scAAV2/1 but not with ssAAV2/1. Indeed, as clearly evidenced by GFP expression in the striatum, which does not contain progenitors, numerous differentiated cells expressed the transgene after scAAV2/1 but not ssAAV2/1 administration (see Fig. 1, 48 hr).

It should be noted that the quantifications performed in the SVZ were limited to the area in which the majority of transgene expression was observed, which represents only approximately one-third of the entire SVZ. If the entirety of the SVZ is to be transduced, two or three injections at different anteroposterior coordinates should be performed. Indeed, SVZ progenitors are found in a region covering approximately 2–3 mm along the anteroposterior (AP) axis and we have previously shown that rAAV2/1 injections into the striatum result in high numbers of *gfp*-expressing cells in a region covering approximately 1–1.5 mm along the AP axis (Bockstael *et al.*, 2008).

AAV vector genomes were shown to remain episomal in rodent (Schnepp *et al.*, 2003), macaque (Afione *et al.*, 1996), and human tissues (Afione *et al.*, 1996; Schnepp *et al.*, 2005). It is therefore expected that when cells proliferate, genomes are diluted and AAV-mediated transgene expression is lost. However, with $10^7$–$10^8$ viral genomes injected, the multiplicity of infection is presumably high at the injection site and in the surrounding area. Hence, numerous rAAV genomes are expected to be present in the nucleus of each transgene-expressing cell. Consequently, GFP$^+$ cells could divide several times before losing transgene expression.

Interference of parvoviruses and in particular AAV and AAV vectors with the cell cycle has repeatedly been reported

(Winocour *et al.*, 1988; Bantel-Schaal and Stohr, 1992; Kube *et al.*, 1997; Fragkos *et al.*, 2008). Reduction of cell numbers in fibroblast primary cultures by wild-type AAV2 virus was shown to be due to accumulation of infected cells in the late S and $G_2$ phases (Winocour *et al.*, 1988; Bantel-Schaal and Stohr, 1992). On the basis of studies with UV-inactivated virus, it has been suggested that viral gene expression was not required (Winocour *et al.*, 1988). Increased levels of the cell cycle inhibitor $p21^{WAF1}$ was demonstrated after AAV2 infection of primary human fibroblasts (Hermanns *et al.*, 1997) as well as primary human keratinocytes (Alam *et al.*, 2006). Recombinant AAV2 vector, devoid of viral coding sequences, was also reported to inhibit fibroblast proliferation (Kube *et al.*, 1997). Kube and colleagues suggested that residual Rep protein attached to the capsid of recombinant AAV might be responsible for this effect (Kube *et al.*, 1997). On the other hand, Fragkos and colleagues (2008) reported that an AAV2 viral DNA sequence within the p5 promoter was responsible for DNA replication inhibition followed by a DNA-damaging response. However, this sequence is not present in AAV vectors.

It was therefore important to assess whether the remarkably rapid and efficient transduction of dividing brain cells could be accompanied by a perturbation of their cell cycle. Indeed, in the present study, a partial inhibition of cell proliferation was observed in the GFP-positive area of the SVZ, shortly after virus infusion. This inhibitory effect was evidenced by two different methods: (1) on the basis of the drastic reduction of the number of double-labeled BrdU-GFP cells (but not of the total number of $BrdU^+$ cells) reaching the OB when BrdU was given immediately after, as compared with immediately before, infection; and (2) the reduction of the proliferative index, consisting of the ratio of the number of dividing ($Ki67^+$) cells 24 hr postinfection and the basal proliferation level as measured by the numbers of cells having incorporated BrdU during 1 day before infection. Altogether, those data suggest that the majority of the infected progenitors stopped proliferating, whereas the uninfected cell population remained unaffected.

We first hypothesized that proliferation inhibition could be related to the vector genome. We report that UV-irradiated AAV2/1 vector similarly reduces the proliferative index, suggesting it is not mediated by transgene expression. The AAV genome has been shown to be the target of DNA repair enzymes (Jurvansuu *et al.*, 2005). However, it was later suggested that a sequence present in the p5 promoter, which is absent in AAV vectors, is necessary for this interaction (Fragkos *et al.*, 2008). On the other hand, single-stranded and self-complementary AAV genomes were shown to interact differently with the DNA double-stranded break repair machinery than single-stranded genomes (Cataldi and McCarty, 2010). In our data, scAAV2/1 and ssAAV2/1 mediate similar proliferation inhibition, in favor of the DNA structure not playing a major role.

In one report, a single-stranded 40-nucleotide G-rich tetrad repeat sequence present in the AAV origin of replication has been shown to induce p53-dependent apoptosis of human embryonic stem cell cultures (Hirsch *et al.*, 2011). This sequence might possibly inhibit progenitor cell division in the present study. However, the TUNEL assay failed to demonstrate increased apoptosis in the AAV2/1-injected SVZ.

Alternatively, the precursor proliferation inhibition effect could be protein mediated. We first excluded that it could be explained by an unspecific high load of proteins as shown by the absence of effect of an equivalent amount of BSA. The inhibitory effect could be mediated by the capsid. In particular, it could be due to a specific peptidic motif inducing a cellular transduction signal pathway leading to the increase of a cell cycle inhibitor such as, for example, $p21^{WAF1}$. In this context, it remains to be determined whether other capsid serotypes have similar effects. Last, it cannot be excluded that Rep proteins produced during the cotransfection of HEK-293T cells could be present in the viral preparations and mediate cell cycle arrest in S phase (Kube *et al.*, 1997; Berthet *et al.*, 2005). Unfortunately, we have no data available about the purity of our vector stocks. We thus cannot exclude the possibility that contaminants are responsible for progenitor proliferation inhibition. However, we observed similar decreases in the proliferative index in the SVZ when injecting similar doses of vector stocks purified by the iodixanol:ion-exchange method (our laboratory) and the $CsCl_2$ gradient method (Laboratoire de Thérapie Génique, Nantes, France) (data not shown). Because it is unlikely that the same contaminants are present in vector batches purified by totally different methods, it is hypothesized that the here-reported absence of effect mediated by bovine albumin in a similar concentration as viral capsids reasonably excludes the possibility of an unspecific effect of high protein load and points to proliferation inhibition being related to an AAV component rather than to a contaminant.

With the aim to recruit neural stem cells toward lesions, it was also important to assess whether migration and differentiation of the SVZ–OB progenitors could be affected by the vector itself. After a transient phase of rapid proliferation, progenitors gradually acquire migrating properties and neuronal markers (Kim *et al.*, 2007). Their final destination and differentiation pattern depend on the initial location of their ancestor neural stem cells (Hack *et al.*, 2005). We show that the percentage of migrating $Dcx^+$ cells relative to the pool of $Mash1^+$ neural precursors was unaltered by viral transduction. Furthermore, the newly generated neurons were located in the OB granular layer, expressed the GAD67 marker of GABAergic neurons, and were TH negative, as expected for cells originating in the SVZ (Smith and Luskin, 1998).

The here-described inhibition of proliferation of immature neuronal cells should be taken into account when interpreting experiments aiming at the recruitment of SVZ neural stem cells by AAV-mediated gene transfer (Henry *et al.*, 2007). It should be noted, however, that this inhibitory effect is transient as demonstrated by the normal BrdU incorporation in the SVZ observed at 1 month postinjection of rAAV2/1 (Henry *et al.*, 2007). The restoration of SVZ proliferative activity after 1 month presumably reflects the dynamics of the SVZ–OB pathway combined with the cellular specificity of rAAV2/1-mediated gene transfer. Indeed, we have shown that after 1 month, the transduced progenitors have migrated to the OB, differentiated, and stopped dividing, whereas the SVZ progenitor population has presumably been reconstituted by the pool of $GFAP^+$ neural stem cells that has not (or poorly) been transduced. Furthermore, the transient inhibition of proliferation did not

seem to interfere with the migration and differentiation of neuroblasts to the OB.

In conclusion, the rapid and efficient transgene expression in SVZ neural precursors is promising concerning the use of scAAV2/1 vectors for the recruitment of SVZ neural progenitors. The observed partial and transient inhibition of proliferation not affecting precursor migration and differentiation will likely not compromise the implementation of this strategy.

## Acknowledgments

The authors thank Dr. V. Depaepe (Université Libre de Bruxelles) for help in analysis of the proliferation index and Dr. R Snyder (University of Florida, Gainesville) for sharing the protocol for qPCR titration of rAAV and Dr L. Pellerin (University of Lausanne) for hosting us for some viral injections. The authors thank the vector core of the University Hospital of Nantes, supported by the Association Française contre les Myopathies (AFM), for the kind gift of some of the ssAAV2/1 vectors used in this study. The authors would like to acknowledge Dr. Frédéric Bollet-Quivogne, Ph.D. (Logistic Scientist F.R.S.-F.N.R.S.) of the Light Microscopy Facility (LiMiF), Université Libre de Bruxelles, Brussels, Belgium, for his support with the confocal imaging presented herein. O.B. was the recipient of a predoctoral fellowship from the Fondation Van Buuren. O.B. was also supported by the French Belgian National Research Foundation (FNRS-Télévie). This work was also supported by a grant from the French Belgian National Research Foundation (FRSM no. 3.4510.06), by grants from the Région Bruxelles-Capitale and the Association Française contre les Myopathies, and from the Swiss National Research Foundation (grant FN 31003A-127177).

## Author Disclosure Statement

The authors state that there are no competing financial interests.

## References

Afione, S.A., Conrad, C.K., Kearns, W.G., *et al.* (1996). *In vivo* model of adeno-associated virus vector persistence and rescue. J. Virol. 70, 3235–3241.

Alam, S., Sen, E., Brashear, H., and Meyers, C. (2006). Adeno-associated virus type 2 increases proteosome-dependent degradation of p21WAF1 in a human papillomavirus type 31b-positive cervical carcinoma line. J. Virol. 80, 4927–4939.

Alam, S., and Meyers, C. (2009). Adeno-associated virus type 2 induces apoptosis in human papillomavirus-infected cell lines but not in normal keratinocytes. J. Virol. 83, 10286–10292.

Alvarez-Buylla, A., and Garcia-Verdugo, J.M. (2002). Neurogenesis in adult subventricular zone. J. Neurosci. 22, 629–634.

Bantel-Schaal, U., and Stohr, M. (1992). Influence of adeno-associated virus on adherence and growth properties of normal cells. J. Virol. 66, 773–779.

Berthet, C., Raj, K., Saudan, P., and Beard, P. (2005). How adeno-associated virus Rep78 protein arrests cells completely in S phase. Proc. Natl. Acad. Sci. U.S.A. 102, 13634–13639.

Bockstael, O., Chtarto, A., Wakkinen, J., *et al.* (2008). Differential transgene expression profiles from rAAV2/1 vectors using the tetON and CMV promoters in the rat brain. Hum. Gene Ther. 19, 1293–1305.

Bockstael, O., Foust, K.D., Kaspar, B., and Tenenbaum, L. (2011). Recombinant AAV delivery to the central nervous system. Methods Mol. Biol. 807, 159–177.

Cataldi, M.P., and McCarty, D.M. (2010). Differential effects of DNA double-strand break repair pathways on single-strand and self-complementary adeno-associated virus vector genomes. J. Virol. 84, 8673–8682.

Chmielnicki, E., Benraiss, A., Economides, A.N., and Goldman, S.A. (2004). Adenovirally expressed noggin and brain-derived neurotrophic factor cooperate to induce new medium spiny neurons from resident progenitor cells in the adult striatal ventricular zone. J. Neurosci. 24, 2133–2142.

Cho, S.R., Benraiss, A., Chmielnicki, E., *et al.* (2007). Induction of neostriatal neurogenesis slows disease progression in a transgenic murine model of Huntington disease. J. Clin. Invest. 117, 2889–2902.

Consiglio, A., Gritti, A., Dolcetta, D., *et al.* (2004). Robust *in vivo* gene transfer into adult mammalian neural stem cells by lentiviral vectors. Proc. Natl. Acad. Sci. U.S.A. 101, 14835–14840.

Craig, C.G., D'sa, R., Morshead, C.M., *et al.* (1999). Migrational analysis of the constitutively proliferating subependyma population in adult mouse forebrain. Neuroscience 93, 1197–1206.

Doetsch, F., Caille, I., Lim, D.A., *et al.* (1999). Subventricular zone astrocytes are neural stem cells in the adult mammalian brain. Cell 97, 703–716.

Duan, D., Yue, Y., Yan, Z., *et al.* (2000). Endosomal processing limits gene transfer to polarized airway epithelia by adeno-associated virus. J. Clin. Invest. 105, 1573–1587.

Fallon, J., Reid, S., Kinyamu, R., *et al.* (2000). *In vivo* induction of massive proliferation, directed migration, and differentiation of neural cells in the adult mammalian brain. Proc. Natl. Acad. Sci. U.S.A. 97, 14686–14691.

Ferrari, F.K., Samulski, T., Shenk, T., and Samulski, R.J. (1996). Second-strand synthesis is a rate-limiting step for efficient transduction by recombinant adeno-associated virus vectors. J. Virol. 70, 3227–3234.

Fisher, K.J., Gao, G.P., Weitzman, M.D., *et al.* (1996). Transduction with recombinant adeno-associated virus for gene therapy is limited by leading-strand synthesis. J. Virol. 70, 520–532.

Fragkos, M., Breuleux, M., Clement, N., and Beard, P. (2008). Recombinant adeno-associated viral vectors are deficient in provoking a DNA damage response. J. Virol. 82, 7379–7387.

Garcia, A.D., Doan, N.B., Imura, T., *et al.* (2004). GFAP-expressing progenitors are the principal source of constitutive neurogenesis in adult mouse forebrain. Nat. Neurosci. 7, 1233–1241.

Geraerts, M., Eggermont, K., Hernandez-Acosta, P., *et al.* (2006). Lentiviral vectors mediate efficient and stable gene transfer in adult neural stem cells *in vivo*. Hum. Gene Ther. 17, 635–650.

Goldman, S.A., Lemmon, V., and Chin, S.S. (1993). Migration of newly generated neurons upon ependymally derived radial guide cells in explant cultures of the adult songbird forebrain. Glia 8, 150–160.

Grimm, D., Kay, M.A., and Kleinschmidt, J.A. (2003). Helper virus-free, optically controllable, and two-plasmid-based production of adeno-associated virus vectors of serotypes 1 to 6. Mol. Ther. 7, 839–850.

Hack, M.A., Saghatelyan, A., de Chevigny, A., *et al.* (2005). Neuronal fate determinants of adult olfactory bulb neurogenesis. Nat. Neurosci. 8, 865–872.

Halbert, C.L., Alexander, I.E., Wolgamot, G.M., and Miller, A.D. (1995). Adeno-associated virus vectors transduce primary cells

much less efficiently than immortalized cells. J. Virol. 69, 1473–1479.

Henry, R.A., Hughes, S.M., and Connor, B. (2007). AAV-mediated delivery of BDNF augments neurogenesis in the normal and quinolinic acid-lesioned adult rat brain. Eur. J. Neurosci. 25, 3513–3525.

Hermanns, J., Schulze, A., Jansen, D., *et al.* (1997). Infection of primary cells by adeno-associated virus type 2 results in a modulation of cell cycle-regulating proteins. J. Virol. 71, 6020–6027.

Hirsch, M.L., Fagan, B.M., Dumitru, R., *et al.* (2011). Viral single-strand DNA induces p53-dependent apoptosis in human embryonic stem cells. PLoS One 6, e27520.

Hughes, S.M., Moussavi-Harami, F., Sauter, S.L., and Davidson, B.L. (2002). Viral-mediated gene transfer to mouse primary neural progenitor cells. Mol. Ther. 5, 16–24.

International Society for BioProcess Technology. (2011). Protocols and test records for AAV2 Reference Material: AAV2_RSS_genome_copy_titration_QPCR. Available at www.isbiotech.org/ReferenceMaterials/pdfs/AAV2_RSS_genome_copy_titration_QPCR.pdf (accessed April 12, 2012).

Jones, K.S., and Connor, B. (2011). Proneural transcription factors Dlx2 and Pax6 are altered in adult SVZ neural precursor cells following striatal cell loss. Mol. Cell. Neurosci. 47, 53–60.

Jurvansuu, J., Raj, K., Stasiak, A., and Beard, P. (2005). Viral transport of DNA damage that mimics a stalled replication fork. J. Virol. 79, 569–580.

Kim, E.J., Leung, C.T., Reed, R.R., and Johnson, J.E. (2007). *In vivo* analysis of Ascl1 defined progenitors reveals distinct developmental dynamics during adult neurogenesis and gliogenesis. J. Neurosci. 27, 12764–12774.

Kim, E.J., Ables, J.L., Dickel, L.K., *et al.* (2011). Ascl1 (Mash1) defines cells with long-term neurogenic potential in subgranular and subventricular zones in adult mouse brain. PLoS One 6, e18472.

Kosaka, K., Aika, Y., Toida, K., *et al.* (1995). Chemically defined neuron groups and their subpopulations in the glomerular layer of the rat main olfactory bulb. Neurosci. Res. 23, 73–88.

Kube, D.M., Ponnazhagan, S., and Srivastava, A. (1997). Encapsidation of adeno-associated virus type 2 Rep proteins in wild-type and recombinant progeny virions: Rep-mediated growth inhibition of primary human cells. J. Virol. 71, 7361–7371.

Lock, M., McGorray, S., Auricchio, A., *et al.* (2010). Characterization of a recombinant adeno-associated virus type 2 Reference Standard Material. Hum. Gene Ther. 21, 1273–1285.

Malik, A.K., Monahan, P.E., Allen, D.L., *et al.* (2000). Kinetics of recombinant adeno-associated virus-mediated gene transfer. J. Virol. 74, 3555–3565.

McCarty, D.M. (2008). Self-complementary AAV vectors: Advances and applications. Mol. Ther. 16, 1648–1656.

McCarty, D.M., Monhan, P.E., and Samulski, R.J. (2001). Self-complementary recombinant adeno-associated virus (scAAV) vectors promote efficient transduction independently of DNA synthesis. Gene Ther. 8, 1248–1254.

McCarty, D.M., Fu, H., Monahan, P.E., *et al.* (2003). Adeno-associated virus terminal repeat (TR) mutant generates self-complementary vectors to overcome the rate-limiting step to transduction *in vivo*. Gene Ther. 10, 2112–2118.

McCown, T.J. (2005). Adeno-associated virus (AAV) vectors in the CNS. Curr. Gene Ther. 5, 333–338.

Ng, R., Govindasamy, L., Gurda, B.L., *et al.* (2010). Structural characterization of the dual glycan binding adeno-associated virus serotype 6. J. Virol. 84, 12945–12957.

Parrish-Aungst, S., Shipley, M.T., Erdelyi, F., *et al.* (2007). Quantitative analysis of neuronal diversity in the mouse olfactory bulb. J. Comp. Neurol. 501, 825–836.

Passini, M.A., Watson, D.J., Vite, C.H., *et al.* (2003). Intraventricular brain injection of adeno-associated virus type 1 (AAV1) in neonatal mice results in complementary patterns of neuronal transduction to AAV2 and total long-term correction of storage lesions in the brains of β-glucuronidase-deficient mice. J. Virol. 77, 7034–7040.

Paxinos G., and Watson C. (1986). *The Rat Brain in Stereotaxic Coordinates* (San Diego, CA, Academic Press).

Reimsnider, S., Manfredsson, F.P., Muzyczka, N., and Mandel, R.J. (2007). Time course of transgene expression after intrastriatal pseudotyped rAAV2/1, rAAV2/2, rAAV2/5, and rAAV2/8 transduction in the rat. Mol. Ther. 15, 1504–1511.

Ricard, J., Salinas, J., Garcia, L., and Liebl, D.J. (2006). EphrinB3 regulates cell proliferation and survival in adult neurogenesis. Mol. Cell. Neurosci. 31, 713–722.

Schnepp, B.C., Clark, K.R., Klemanski, D.L., *et al.* (2003). Genetic fate of recombinant adeno-associated virus vector genomes in muscle. J. Virol. 77, 3495–3504.

Schnepp, B.C., Jensen, R.L., Chen, C.L., *et al.* (2005). Characterization of adeno-associated virus genomes isolated from human tissues. J. Virol. 79, 14793–14803.

Smith, C.M., and Luskin, M.B. (1998). Cell cycle length of olfactory bulb neuronal progenitors in the rostral migratory stream. Dev. Dyn. 213, 220–227.

Tenenbaum, L., Hamdane, M., Pouzet, M., *et al.* (1999). Cellular contaminants of adeno-associated virus vector stocks can enhance transduction. Gene Ther. 6, 1045–1053.

Thomas, C.E., Storm, T.A., Huang, Z., and Kay, M.A. (2004). Rapid uncoating of vector genomes is the key to efficient liver transduction with pseudotyped adeno-associated virus vectors. J. Virol. 78, 3110–3122.

Wang, C., Wang, C.M., Clark, K.R., and Sferra, T.J. (2003). Recombinant AAV serotype 1 transduction efficiency and tropism in the murine brain. Gene Ther. 10, 1528–1534.

Winocour, E., Callaham, M.F., and Huberman, E. (1988). Perturbation of the cell cycle by adeno-associated virus. Virology 167, 393–399.

Wu, P., Ye, Y., and Svendsen, C.N. (2002). Transduction of human neural progenitor cells using recombinant adeno-associated viral vectors. Gene Ther. 9, 245–255.

Yanez-Munoz, R.J., Balaggan, K.S., MacNeil, A., *et al.* (2006). Effective gene therapy with nonintegrating lentiviral vectors. Nat. Med. 12, 348–353.

Zolotukhin, S., Byrne, B.J., Mason, E., *et al.* (1999). Recombinant adeno-associated virus purification using novel methods improves infectious titer and yield. Gene Ther. 6, 973–985.

Address correspondence to:
*Dr. Olivier Bockstael*
*Laboratory of Experimental Neurosurgery/IRIBHM, CP602*
*U.L.B.-Hôpital Erasme*
*1070 Brussels*
*Belgium*

*E-mail:* olivier.bockstael@ulb.ac.be

Received for publication December 5, 2011;
accepted after revision March 9, 2012.

Published online: April 3, 2012.